AGU ADVANCING EARTH AND SPACE SCIENCES

AGU Advances

RESEARCH ARTICLE
10.1029/2023AV000964

The 8-Year Solar Cycle During the Maunder Minimum

Limei Yan[1,2], Fei He[1,2], Xinan Yue[1,2], Yong Wei[1,2], Yuqi Wang[1,2], Si Chen[3], Kai Fan[1,2], Hui Tian[4,5], Jiansen He[4], Qiugang Zong[4], and Lidong Xia[6]

[1]Key Laboratory of Earth and Planetary Physics, Institute of Geology and Geophysics, Chinese Academy of Sciences, Beijing, China, [2]College of Earth and Planetary Sciences, University of Chinese Academy of Sciences, Beijing, China, [3]Aerospace Information Research Institute, Chinese Academy of Sciences, Beijing, China, [4]School of Earth and Space Sciences, Peking University, Beijing, China, [5]Key Laboratory of Solar Activity and Space Weather, National Space Science Center, Chinese Academy of Sciences, Beijing, China, [6]Shandong Provincial Key Laboratory of Optical Astronomy and Solar-Terrestrial Environment, School of Space Science and Physics, Shandong University, Weihai, China

Abstract The presence of grand minima, characterized by significantly reduced solar and stellar activity, brings a challenge to the understanding of solar and stellar dynamo. The Maunder Minimum (1645–1715 AD) is a representative grand solar minimum. The cyclic variation of solar activity, especially the cycle length during this period, is critical to understand the solar dynamo but remains unknown. By analyzing the variations in solar activity-related equatorial auroras recorded in Korean historical books in the vicinity of a low-intensity paleo-West Pacific geomagnetic anomaly, we find clear evidence of an 8-year solar cycle rather than the normal 11-year cycle during the Maunder Minimum. This result provides a key constraint on solar dynamo models and the generation mechanism of grand solar minima.

Plain Language Summary The solar cycle length during the Maunder Minimum is vital for understanding the appearance of the grand solar minimum. However, owing to the limited data quality of the currently used solar activity proxies, the cyclic variation of solar activity still needs to be explored during the Maunder minimum. Here, we show definitive observational evidence of an 8-year solar cycle during the Maunder Minimum using historical observations of equatorial aurorae. The 8-year solar cycle length found here provides a pivotal clue to understanding the origin and predictability of the grand solar minimum.

1. Introduction

Certain cyclic fluctuations of solar activity have important clues to the physical nature of solar dynamo process (Charbonneau, 2020). The resultant solar output variations significantly impact space climate and space weather on Earth and the solar system (Temmer, 2021). The most pronounced quasi-periodic variation of solar activity is the Schwabe cycle (Usoskin, 2017), which varies between 9 and 14 years with an average of ∼11 years. The amplitude of the Schwabe cycle is fluctuating and is sometimes exceptionally highly depressed when the Sun comes into a grand minimum (Usoskin, 2017) which is usually attributed to a distinct solar dynamo mode (Käpylä et al., 2016; Usoskin et al., 2014). A well-known grand minimum in solar activity is the Maunder Minimum (Eddy, 1976) from 1645 to 1715 AD, during which sunspots are exceedingly rare, the total solar irradiance is declined (Shapiro et al., 2011), and the solar wind keeps blowing at a lower speed (Cliver et al., 1998; Lockwood et al., 2014; Owens et al., 2017). The grand minimum is not unique to solar activity, but also appears in the activity of other stars (Judge & Saar, 2007). The Maunder Minimum is usually considered as the archetype of the grand minima in solar and stellar activity and is key to understand the solar and stellar dynamo.

Characterizing the periodicity of solar activity during the Maunder Minimum will benefit the understanding of the nature of solar dynamo. Lots of data sets have been used to investigate the cyclic activity during the Maunder Minimum, such as the sunspot observations (Nagovitsyn, 2007; Ribes & Nesme-Ribes, 1993; Vaquero et al., 2015), the cosmogenic radionuclide data sets (Beer et al., 1998; Miyahara et al., 2004; Poluianov et al., 2014; Usoskin et al., 2021), and the polar aurora at high latitudes (Schlamminger, 1990; Schröder, 1992; Silverman, 1992). However, the currently used data sets give controversial results on the solar cycle length during the Maunder Minimum, which has been suggested to be a normal 11-year (Beer et al., 1998; Poluianov et al., 2014; Schlamminger, 1990; Schröder, 1992), a lengthened ∼13–16-year (Miyahara et al., 2004; Silverman, 1992), or a shortened 9 ± 1 year solar cycle which is uncertain because of the unclear sunspot situation around some years (Vaquero et al., 2015). Obviously, limited by the quality of solar activity proxies, there is still no consensus on

Limei Yan, Fei He and Xinan Yue contributed equally to this work.

Peer Review The peer review history for this article is available as a PDF in the Supporting Information.

Key Points:

- Give a definitive observational evidence of an 8-year solar cycle during Maunder Minimum
- The distinct solar dynamo during the Maunder Minimum is not chaotic
- A consistent dynamo explanation is a superposition of the dipole (22 years) and the quadrupole (∼13–15 years) with nearly equal amplitude

Supporting Information:

Supporting Information may be found in the online version of this article.

Correspondence to:

Y. Wei,
weiy@mail.iggcas.ac.cn

Citation:

Yan, L., He, F., Yue, X., Wei, Y., Wang, Y., Chen, S., et al. (2023). The 8-year solar cycle during the Maunder Minimum. *AGU Advances*, *4*, e2023AV000964. https://doi.org/10.1029/2023AV000964

Received 24 MAY 2023
Accepted 12 SEP 2023

Author Contributions:

Conceptualization: Yong Wei
Data curation: Yuqi Wang, Si Chen
Formal analysis: Limei Yan, Fei He, Xinan Yue
Funding acquisition: Limei Yan, Fei He, Yong Wei, Hui Tian
Investigation: Limei Yan, Fei He, Xinan Yue
Methodology: Limei Yan, Fei He, Xinan Yue
Project Administration: Yong Wei
Software: Limei Yan, Fei He, Xinan Yue

Supervision: Yong Wei
Validation: Limei Yan, Fei He, Xinan Yue, Kai Fan, Hui Tian, Jiansen He, Qiugang Zong, Lidong Xia
Visualization: Limei Yan, Fei He, Xinan Yue
Writing – original draft: Limei Yan, Fei He, Xinan Yue
Writing – review & editing: Limei Yan, Fei He, Xinan Yue, Yong Wei, Yuqi Wang, Si Chen, Kai Fan, Hui Tian, Jiansen He, Qiugang Zong, Lidong Xia

the cyclic variations during the Maunder Minimum, especially the cycle length, which is crucial to constrain the solar dynamo model.

Some dynamo models have reproduced Maunder Minimum-like behavior with no emerged magnetic flux in one or both solar hemisphere(s). However, these models usually give divergent cycle periods during the grand minima. For example, Passos et al. (2014) showed that the cycle period during grand minima-like episodes is similar to that of normal activity phases, whereas Karak and Miesch (2018) suggested considerable changes in the cycle period. The controversial cycle period of the Maunder Minimum motivates us to seek a reliable solar activity data set throughout the episode to pin down its exact value.

On the Earth, there are two types of auroral displays that are closely related to solar activity. The first is the polar aurora and the second is the red equatorial aurora. In Earth's high-latitude regions, energetic particles precipitating along the dipolar geomagnetic field lines collide and excite the atoms and molecules in the atmosphere to generate polar auroras (Ni et al., 2016), which have long been considered as optical manifestation of the solar activity in near-Earth space (Gorney, 1990; Silverman, 1983). Traditionally, auroras are just observed in the high-latitude oval region surrounding the geomagnetic poles and are occasionally observed in low latitudes during extreme space weather events (Figure 1). However, past polar aurora records during the Maunder Minimum did not give a convincing, definitive conclusion about the solar cycle length due to the small sample size. Hence, to explore the periodicity of solar activity during the Maunder Minimum, we concentrated our studies on a particular class of red equatorial auroras compiled from historical books (He et al., 2020; Wang et al., 2021) and found a significant ∼8-year cycle, providing important clues for future investigation of solar dynamo during the GM.

In the low-latitude region, if the geomagnetic field intensity is low enough to allow energetic particles to penetrate deep into the atmosphere, such as in the South Atlantic Anomaly (SAA), a special dynamic red equatorial aurora can occur during geomagnetic storms (He et al., 2020) and thus is closely related to solar activity. The geomagnetic West Pacific Anomaly (WPA), which is a low-intensity geomagnetic anomaly in the West Pacific region as revealed by several geomagnetic models (Campuzano et al., 2019; Constanble et al., 2016; He et al., 2021; Jackson et al., 2000), existed between ∼1500 and 1800 AD, covering the Maunder Minimum (Figure 1). The geomagnetic field intensity in the WPA is low enough to allow energetic particles to penetrate deep into the atmosphere and excite dynamic equatorial aurora during storm time, and therefore can be used as a proxy of the solar activity. This kind of auroras during the Maunder Minimum was fortunately observed by the naked eyes of ancient Korean professional astronomers and routinely recorded on daily resolution, from which a large equatorial auroral catalog was compiled (Wang et al., 2021), providing a unique way to investigate solar activity during the Maunder Minimum.

2. Data and Methods

2.1. A Catalog of Ancient Aurora in the WPA

There exist several frequently used auroral list in the past, which have been created by the community for different purposes and therefore show different emphasis on either origin of ancient books or geographic location or span of time (Dai & Chen, 1980; Hayakawa et al., 2017; Lee et al., 2004; Lockwood & Barnard, 2015; Stephenson & Willis, 2008; Usoskin et al., 2015; Willis et al., 1996, 2007; Yau et al., 1995; Zhang, 1985). In a recent teamwork, we compiled a new auroral catalog from ancient Korean historical books of the Koryo-Sa, the Choson Wangjo Sillok and the Seungjeongwon Ilgi through automatic retrieval from the digital books with formatted keywords and manual confirmation for each record (Wang et al., 2021). The new catalog contains a considerably greater number of auroral observations than previous lists. Our study has presented an opportunity to confirm that most, or perhaps all, of the auroral observations south of the Korean peninsula were equatorial auroras resulting from energetic particle precipitation into the atmosphere facilitated by the WPA during that period (He et al., 2020, 2021).

The red aurora usually occurs in a height range of 200∼400 km (Aryal et al., 2018; He et al., 2020, 2021). The maximum visible region from the ancient observatory in Seoul, Korea for this height range is shown as the cyan and pink circles respectively in Figure 1. The configuration of the geomagnetic field is interesting during the Maunder Minimum. First, there is a low-intensity WPA southward of the Korea peninsula and the equatorial auroral generated in this region is visible to an observer at Seoul. Second, according to the CALS10k.2 geomagnetic field

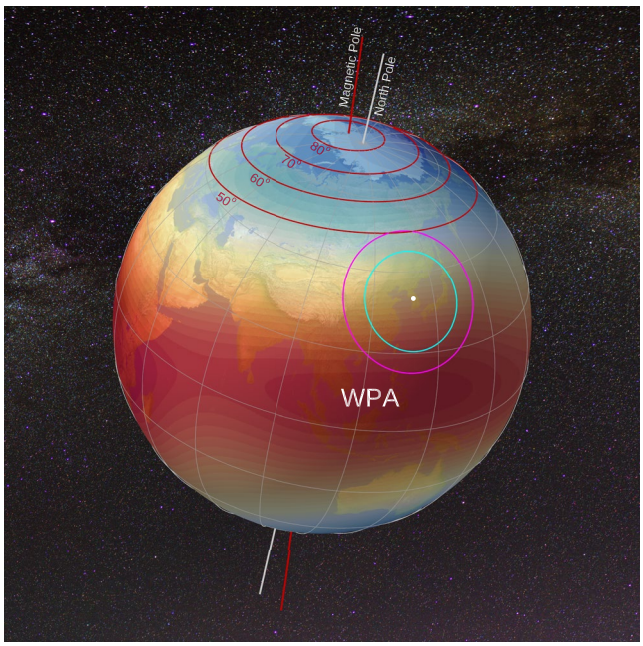

Figure 1. Illustration of auroral observations from Korean peninsula. The ancient observatory at Seoul, South Korea, is denoted by the white dot. The magenta color shows the core of the paleo-West Pacific Anomaly (WPA) of low magnetic intensity. The Earth rotation axis and the geomagnetic axis are denoted by the black and red lines, respectively. The geomagnetic axis is calculated with the CALS10k.2 model at 1645 (Constable et al., 2016). The red circles represent the geomagnetic latitudes above 50° with an increment of 10°, also calculated with the CALS10k.2 model. The pink and cyan circles show the visible range at Seoul for altitudes of 400 and 200 km, respectively.

model (Constable et al., 2016), the Magnetic Pole is close to the North Pole during the Maunder Minimum and the regions below geomagnetic latitudes of 50° is visible to an observer at Seoul. Therefore, both polar aurora and red equatorial aurora could be observed at Seoul. For the polar aurora, only during strong geomagnetic storms (Kp ≥ 7), and thus strong solar eruptions (such as strong coronal mass ejections), that the boundary of polar aurora could expand to geomagnetic latitudes below 50° (according to National Oceanic and Atmospheric Administration Space Weather Scales). However, Usoskin et al. (2015) have shown from a combination of auroral catalogs that 1715 polar auroral observations were seen in Europe below geomagnetic latitudes of 50°, soon after the end of the Maunder Minimum, but none were recorded during the Maunder Minimum, strongly supporting that the ancient Korean observations were of red midlatitude/equatorial aurora. For the red equatorial auroral, energetic particle precipitation in the WPA during a small geomagnetic storm can make the aurora visible to naked eye (He et al., 2020). During 1620–1810 AD, there are 1406 aurora records, 1012 of which are red equatorial aurora records observed in the southern nocturnal sky of Korea Peninsula (south, southwest, and southeast). In this study, we just focus on the red equatorial aurora records.

Although the auroras were recorded daily, we bin the data by temporal resolution in two different ways in this study. The first is 10-year resolution data which denotes the number of days with auroral records during each 10-year interval (see Figure S1c in Supporting Information S1). The second is 1-year resolution which denotes the number of days with equatorial auroral records during each year (Figure 2b). At the beginning of the Maunder Minimum, the magnetic intensity of the WPA began to increase (see Figures S1b and S1d in Supporting Information S1), strengthening the shielding of magnetic field to the energetic particles, and thus leading to the decreasing trend of red equatorial aurora occurrence after 1645 AD. After 1700 AD, even there is a decrease in magnetic intensity as deduced from the aurora records (Korte et al., 2009), the intensity is not so low as that during the first half of the Maunder Minimum. Therefore, the number of auroral records kept at a low level during the second half of the Maunder Minimum.

2.2. Lomb-Scargle Spectral Analysis

The Lomb-Scargle (LS) spectral analysis is a well-known algorithm for detecting and characterizing periodic signals in unevenly sampled data (Press & Rybicki, 1989) after the pioneer work by Lomb (1976) and Scargle (1982). It is equivalent to the least square fitting of the sine waves to the data under the theory of Bayes. In our study, since the aurora occurrence records distribute unevenly versus time, determining periods in such series is not directly possible with methods such as Fast Fourier Transform and may require some degree of interpolation to fill in gaps. Therefore, Lomb-Scargle spectral analysis was applied in the paper. Specifically, for a time series of aurora records with N elements, $x(k)$, the Lomb-Scargle periodogram as a function of frequency f is derived by the following formula (Lomb, 1976; Scargle, 1982):

$$\mathrm{LSP}(f)=\frac{1}{2\sigma^2}\left\{\frac{\left[\sum_{k=1}^{N}\left(x(k)-\overline{x}\right)\cos(2\pi f(t(k)-\tau))\right]^2}{\sum_{k=1}^{N}\cos^2(2\pi f(t(k)-\tau))}+\frac{\left[\sum_{k=1}^{N}\left(x(k)-\overline{x}\right)\sin(2\pi f(t(k)-\tau))\right]^2}{\sum_{k=1}^{N}\sin^2(2\pi f(t(k)-\tau))}\right\} \quad (1)$$

where $t(k)$ is the date corresponding to aurora occurrence, $\overline{x}$ and σ^2 are respectively the mean and the variance of the aurora record time series. To insure the time invariance of the computed spectrum, the time shift τ is defined as follows:

$$\tau=\frac{1}{2(2\pi f)}\tan^{-1}\frac{\sum_{k=1}^{N}\sin(2(2\pi f)t(k))}{\sum_{k=1}^{N}\cos(2(2\pi f)t(k))} \quad (2)$$

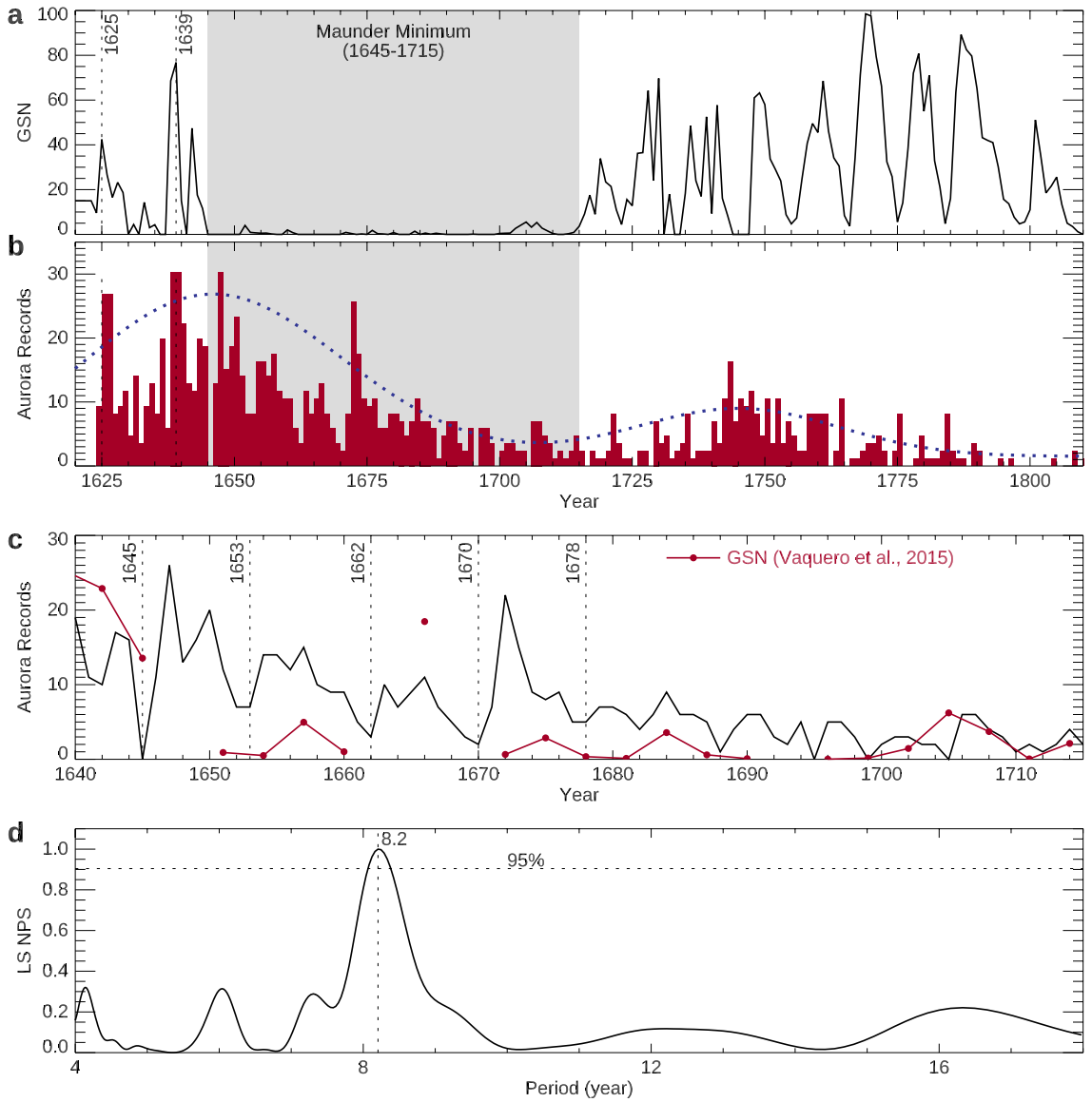

Figure 2. Evolutions of solar activity and equatorial aurora records. (a) Annual group sunspot number (GSN) from 1620 to 1810 AD. (b) Annual equatorial aurora records from 1620 to 1810 AD. The dashed blue curve denotes a multipeak Gaussian function fit of an envelope of the red equatorial aurora occurrence. (c) Zoom-in view of the red equatorial aurora occurrence during the period from 1640 to 1715 AD. The sporadic records of GSN deduced from the active-day statistics (Vaquero et al., 2015) are overplotted. (d) The LS normalized power spectrum (NPS) of the red equatorial aurora occurrence during the period from 1640 to 1720 AD. The horizontal dashed line indicates the 95% possibility of detection level line, and the vertical dashed line marks the peak at 8.2 years.

In the paper, the Lomb-Scargle periodogram results were shown in Figure 2d. Furthermore, in Figure 2d we also show the 95% possibility of detection level line, which means that the normalized power spectral density larger than the value represented by the line has a 95% probability that a period in the spectrum is not due to random fluctuations.

3. Results

During the Maunder Minimum, the low-intensity WPA centered at South China Sea (Figure 1) provided the conditions necessary to produce equatorial aurora, analogous to that seen in the SAA. Northward of the WPA, ancient dynasties in China, Korea, and Japan preserved numerous official/unofficial astronomical records, of particular importance here being the official daily records in ancient Korea around the seventeenth century. The most frequently recorded night sky glow was described as "vapors like fire light," which has been widely

interpreted as red auroras (Hayakawa et al., 2017; Stephenson & Willis, 2008). Recently, Wang et al. (2021) systematically searched the Korean historical books and established a large catalog containing 2013 auroral records from 1012 AD to 1811 AD (see Figure S1 in Supporting Information S1). A total of 1012 equatorial aurora records observed in the southern nocturnal sky from 1620 to 1810 are used in this study. The comparisons between the annual auroral records and the annual group sunspot number (GSN) (Hoyt & Schatten, 1998) are shown in Figure 2.

An increased solar activity and/or a locally weakened magnetic field can both contribute to the enhanced particle precipitation that causes the dynamic equatorial auroras. It has been demonstrated that, at the centennial time scale, the red equatorial aurora occurrence (i.e., the number of days with red equatorial aurora records in each year) is modulated by the temporal variation of the magnetic intensity in the WPA (He et al., 2021), as illustrated by the blue dashed line in Figure 2b. Therefore, the red equatorial aurora occurrence after the Maunder Minimum (after 1715) did not recover to a higher level as that of the GSN, and this is mainly owing to the recovery of the WPA (See Data and Methods, and Figure S1 in Supporting Information S1). The secular change in the intrinsic geomagnetic field (e.g., geomagnetic pole shift) can also influence the auroral sightings in the polar region (Lockwood & Barnard, 2015). Combining the auroral records with other auroral catalogs (Usoskin et al., 2015), the Maunder Minimum can be defined as a real minimum in auroral occurrence. Besides the variations on the centennial timescale, the annual aurora records also exhibit fluctuations close to the Schwabe cycle scale, which we will focus on to investigate the relation between the red equatorial aurora and solar activity.

Before the Maunder Minimum (1620–1645 AD), there are two significant peaks in the GSN as indicated by the two vertical dashed lines at 1625 and 1639 AD (Figure 2a), respectively. Interestingly, there are also two peaks in the red equatorial aurora occurrence (Figure 2b), perfectly corresponding to the two GSN peaks. Furthermore, both the red equatorial aurora occurrence and the GSN show an extended minimum between 1625 and 1639 AD. The good consistency of the variations of the red equatorial aurora occurrence and the GSN before the Maunder Minimum indicates that the red equatorial aurora can be used as a solar activity proxy to characterize the cyclic variations during the Maunder Minimum.

The variation of the red equatorial aurora occurrence during the Maunder Minimum is shown in Figure 2c. The sunspot record is extremely sparse during this period, showing no prominent, continuous cyclic variations from 1645 to 1670. The red equatorial aurora occurrence exhibits four prominent successive ∼8-year cyclic variations during the first half of the Maunder Minimum, which lasted at least for four stable cycles with the cycle minima at 1645, 1653, 1662, 1670, and 1678 AD (Figure 2c), respectively. The corresponding cycle lengths are 8, 9, 8, and 8 years, respectively, with an average of 8.25 years. It is noted that the 8-year cyclic variation is mainly remarkable during the descent into the Maunder Minimum and not later in the Maunder Minimum. It suggests that the solar activity behavior might have changed as the grand minimum progressed, which is consistent with the solar activity declination as revealed by the cosmogenic isotope abundances (Lockwood et al., 2011). It could also be due to low occurrence of the red equatorial aurora in the vicinity of the enhancement of the magnetic field strength in the WPA (He et al., 2021) (See Figure S1 in Supporting Information S1). Nevertheless, the Lomb-Scargle (LS) normalized power spectrum for the equatorial auroral records from 1640 to 1720 in Figure 2d further reveals that the dominant period is 8.2 years during the Maunder Minimum. These results indicate that, during the Maunder Minimum, the solar dynamo cycle was not switched off but entered another cyclic mode.

4. Conclusions

Purely in terms of cycle length, the 8-year cycle found here is close to the 9 ± 1 year inferred from the sunspots (Vaquero et al., 2015). However, there are significant differences. The sunspot data sets cannot distinguish each cycle precisely and only give a rough estimation of the cycle length with a large uncertainty. However, the 8-year cycle shown here is stable and reliable, with each cycle's minima precisely identified. The 8-year cycle provides a new constraint on the solar dynamo model and is crucial for understanding the generation of the GM. In addition, the identified individual cycles are essential for studying the solar-terrestrial relations during the Maunder Minimum.

Such a remarkably stable ∼8-year cyclic variation lasting for four cycles could exclude the chaotic nature of the solar dynamo during the Maunder Minimum. In normal solar activity beyond the GM, the solar cycle amplitude

is inversely correlated with the cycle length (Solanki et al., 2002). Following the inverse relationship between the cycle amplitude and length, the highly depressed solar activity during the Maunder Minimum should have a lengthened cycle. However, the 8-year cycle reported here contradicts this scenario. Therefore, the 8-year cycle reported here differs from the normal ∼11-year Schwabe cycle fluctuating between 9 and 14 years and indicates the different solar dynamo during the Maunder Minimum.

The 8-year cycle is not unique for the Maunder Minimum. The cyclic variation around 8 years also appears in modern solar observations beyond the Maunder Minimum. For example, the hemispheric asymmetry of solar activity usually shows ∼8–9-year periodic variations (Ballester et al., 2005; De Paula et al., 2022; Deng et al., 2016). Besides, a weak ∼8-year period also appears in the modern sunspot data sets (Krivova & Solanki, 2002; Zhu & Jia, 2018) and the solar 10.7 cm radio flux (Roy et al., 2019). Taking advantage of the highly hemispheric asymmetric of sunspot activity with almost all sunspots confined to the southern hemisphere during the Maunder Minimum (Ribes & Nesme-Ribes, 1993), the ∼8–9-year cycle in the hemispheric asymmetry of solar activity gives clues to understand the solar dynamo during the Maunder Minimum.

One consistent explanation of the ∼8-year cycle reported here is the superposition of the dipolar mode with a period around 22 years and the quadrupolar mode with a period around 13–15 years (Schüssler & Cameron, 2018), which is proposed to explain the ∼8–9-year periodic variations in hemispheric asymmetry of solar activity. Beyond the GM, the solar activity is dominated by the dipolar mode (∼22 years). For example, from 1874 to 2016, the amplitude of the quadrupolar mode is only ∼0.17 that of the dipolar mode (Kitchatinov, 2022). Beyond the GM, the superposition of the dominant ∼22-year periodic dipolar mode and the subdominant ∼13–15-year periodic quadrupolar mode leads to the cyclic variations of solar activity dominated by the ∼11-year Schwabe cycle with a weak north-south asymmetry exhibiting a period of ∼8–9 years. When the dipolar mode and the quadrupolar mode have nearly equal amplitudes (Sokoloff & Nesme-Ribes, 1994), the superposition of them will lead to the solar activity being confined almost only to one hemisphere, which is just the situation during the Maunder Minimum. The ∼8-year solar cycle during the Maunder Minimum likely results from a combination of the dipolar mode (22 years) and the quadrupolar mode (∼13–15 years) with nearly equal amplitude (see Figure S2 and Text S1 in Supporting Information S1).

Another candidate source for the shorter cycle length (∼8 years) reported here is a meridional circulation flow faster than usual. The surface meridional circulation flow transports the magnetic field to the poles reversing the old polar field and building up the new polar field, the strength of which is strongly correlated with the amplitude of the next solar cycle (Jiang et al., 2018). The meridional circulation counterflow near the base of the solar convection zone is a primary driver of the cycle length, with the meridional circulation flow speed inversely correlated with the solar cycle length (Dikpati & Charbonneau, 1999; Hathaway et al., 2003; Yeates et al., 2008). If a faster meridional circulation flow sweeps both the positive and negative polarity sunspots to the polar regions (e.g., in the surface flux transport model), lower net flux would be available for reversing the old polar fields and building up weaker polar fields of the new cycle (Hathaway & Rightmire, 2010; Nandy et al., 2011), leading to weaker and shorter cycles. Therefore, a meridional circulation flow faster than usual has the possibility to induce a shorter cycle length (∼8 years) with lower amplitude.

Finally, it is noted that it is the open solar flux (OSF) that links the photospheric field changes corresponding to sunspots and the auroral observations. Here we assume that the present-day relationship between aurorae and sunspots pertains to the Maunder Minimum. The assumption might not hold because of other sources, for example, the loss rate of OSF (Owens & Lockwood, 2012). Different sources of the cyclic variations in the Maunder Minimum to those seen before and after the Maunder Minimum are supported by the observed positive-correlation between the sunspot number and the cosmogenic isotope abundances (Owens et al., 2012; Usoskin et al., 2015), rather than the anti-correlation during normal solar cycles. Eclipse observations (Hayakawa et al., 2021) and numerical simulations (Riley et al., 2015) also showed some evidence that the form of the corona and hence the OSF was different during the Maunder Minimum. It remains to be discovered whether the present-day relationship between aurorae and sunspots can be applied during the Maunder Minimum.

Conflict of Interest

The authors declare no conflicts of interest relevant to this study.

Data Availability Statement

The ancient Korean auroral records used in this study (Wang et al., 2021) are publicly available in He and Wei (2021). The annual group sunspot number (Hoyt & Schatten, 1998) are publicly available at the World Data Center for Sunspot Index and Long-term Solar Observations (WDC-SILSO, 1620–1810). The GSN deduced from the active-day statistics are available in Vaquero et al. (2015). The CALS10k.2 geomagnetic model are available in Constable et al. (2016).

Acknowledgments
The authors greatly appreciate Dr. Jie Jiang at Beihang University for valuable discussions. National Natural Science Foundation of China 42241106(Y.W.), 42074207(L.Y.), 42222408 (F.H.), 11825301(H.T.); Youth Innovation Promotion Association of Chinese Academy of Sciences, 2021064 (L.Y.), Y2021027 (F.H.); Key Research Program of the Institute of Geology & Geophysics, CAS IGGCAS-201904 (Y.W.).

References

Aryal, S., Finn, S. C., Hewawasam, K., Maguire, R., Geddes, G., Cook, T., et al. (2018). Derivation of the energy and flux morphology in an aurora observed at midlatitude using multispectral imaging. *Journal of Geophysical Research: Space Physics*, *123*(5), 4257–4271. https://doi.org/10.1029/2018JA025229

Ballester, J. L., Oliver, R., & Carbonell, M. (2005). The periodic behaviour of the North-South asymmetry of sunspot areas revisited. *Astronomy & Astrophysics*, *431*(2), L5–L8. https://doi.org/10.1051/0004-6361:200400135

Beer, J., Tobias, S., & Weiss, N. (1998). An active Sun throughout the Maunder Minimum. *Solar Physics*, *181*(1), 237–249. https://doi.org/10.1023/A:1005026001784

Campuzano, S. A., Gómez-Paccard, M., Pavón-Carrasco, F. J., & Osete, M. L. (2019). Emergence and evolution of the South Atlantic Anomaly revealed by the new paleomagnetic reconstruction SHAWQ2k. *Earth and Planetary Science Letters*, *512*, 17–26. https://doi.org/10.1016/j.epsl.2019.01.050

Charbonneau, P. (2020). Dynamo models of the solar cycle. *Living Reviews in Solar Physics*, *17*(1), 4. https://doi.org/10.1007/s41116-020-00025-6

Cliver, E. W., Boriakoff, V., & Feynman, J. (1998). Solar variability and climate change: Geomagnetic aa index and global surface temperature. *Geophysical Research Letters*, *25*(7), 1035–1038. https://doi.org/10.1029/98GL00499

Constable, C., Korte, M., & Panovska, S. (2016). Persistent high paleosecular variation activity in southern hemisphere for at least 10000 years. *Earth and Planetary Science Letters*, *453*, 78–86. https://doi.org/10.1016/j.epsl.2016.08.015. The Fortran source code and the Gauss coefficients for the CALS10k.2 model described in this work can be publicly available at https://www.gfz-potsdam.de/en/section/geomagnetism/data-products-services/mag-models

Dai, N. Z., & Chen, M. D. (1980). Chronology of northern light in history of China, Korea and Japan: From the legendary period to 1747AD. *Kejishiwenji*, *6*, 87–146.

Deng, L. H., Xiang, Y. Y., Qu, Z. N., & An, J. M. (2016). Systematic regularity of hemispheric sunspot areas over the past 140 years. *The Astronomical Journal*, *151*(3), 70. https://doi.org/10.3847/0004-6256/151/3/70

De Paula, V., Curto, J. J., & Oliver, R. (2022). The cyclic behaviour in the N–S asymmetry of sunspots and solar plages for the period 1910 to 1937 using data from Ebro catalogues. *Monthly Notices of the Royal Astronomical Society*, *512*(4), 5726–5742. https://doi.org/10.1093/mnras/stac424

Dikpati, M., & Charbonneau, P. (1999). A Babcock-Leighton flux transport dynamo with solar-like differential rotation. *The Astrophysical Journal*, *518*(1), 508–520. https://doi.org/10.1086/307269

Eddy, J. A. (1976). Maunder minimum. *Science*, *192*(4245), 1189–1202. https://doi.org/10.1126/science.192.4245.1189

Gorney, D. J. (1990). Solar cycle effects on the near-Earth space environment. *Reviews of Geophysics*, *28*(3), 315–336. https://doi.org/10.1029/RG028i003p00315

Hathaway, D. H., Nandy, D., Wilson, R. M., & Reichmann, E. J. (2003). Evidence that a deep meridional flow sets the sunspot cycle period. *The Astrophysical Journal*, *589*(1), 665–670. https://doi.org/10.1086/374393

Hathaway, D. H., & Rightmire, L. (2010). Variations in the Sun's meridional flow over a solar cycle. *Science*, *327*(5971), 1350–1352. https://doi.org/10.1126/science.1181990

Hayakawa, H., Iju, T., Murata, K., & Besser, B. P. (2021). Daniel Mögling's sunspot observations in 1626–1629: A manuscript reference for the solar activity before the Maunder Minimum. *The Astrophysical Journal*, *909*(2), 194. https://doi.org/10.3847/1538-4357/abdd34

Hayakawa, H., Tamazawa, H., Ebihara, Y., Miyahara, H., Kawamura, A. D., Aoyama, T., & Isobe, H. (2017). Records of sunspots and aurora candidates in the Chinese official histories of the Yuán and Míng dynasties during 1261–1644. *Publications of the Astronomical Society of Japan*, *69*(4). https://doi.org/10.1093/pasj/psx045

He, F., & Wei, Y. (2021). Ancient Korean aurora records [Dataset]. Figshare. https://doi.org/10.6084/m9.figshare.14471154

He, F., Wei, Y., Maffei, S., Livermore, P. W., Davies, C. J., Mound, J., et al. (2021). Equatorial auroral records reveal dynamics of the paleo-West Pacific geomagnetic anomaly. *Proceedings of the National Academy of Sciences of the United States of America*, *118*(20), e2026080118. https://doi.org/10.1073/pnas.2026080118

He, F., Wei, Y., & Wan, W. (2020). Equatorial aurora: The aurora-like airglow in the negative magnetic anomaly. *National Science Review*, *7*(10), 1606–1615. https://doi.org/10.1093/nsr/nwaa083

Hoyt, D. V., & Schatten, K. H. (1998). Group sunspot numbers: A new solar activity reconstruction. *Solar Physics*, *179*(1), 189–219. https://doi.org/10.1023/A:1005007527816

Jackson, A., Jonkers, A. R., & Walker, M. R. (2000). Four centuries of geomagnetic secular variation from historical records. *Philosophical Transactions of the Royal Society of London, Series A: Mathematical, Physical and Engineering Sciences*, *358*(1768), 957–990. https://doi.org/10.1098/rsta.2000.0569

Jiang, J., Wang, J. X., Jiao, Q. R., & Cao, J. B. (2018). Predictability of the solar cycle over one cycle. *The Astrophysical Journal*, *863*(2), 159. https://doi.org/10.3847/1538-4357/aad197

Judge, P. G., & Saar, S. H. (2007). The outer solar atmosphere during the Maunder Minimum: A stellar perspective. *The Astrophysical Journal*, *663*(1), 643–656. https://doi.org/10.1086/513004

Käpylä, M. J., Käpylä, P. J., Olspert, N., Brandenburg, A., Warnecke, J., Karak, B. B., & Pelt, J. (2016). Multiple dynamo modes as a mechanism for long-term solar activity variations. *Astronomy & Astrophysics*, *589*, A56. https://doi.org/10.1051/0004-6361/201527002

Karak, B. B., & Miesch, M. (2018). Recovery from Maunder-like grand minima in a Babcock–Leighton solar dynamo model. *The Astrophysical Journal Letters*, *860*(2), L26. https://doi.org/10.3847/2041-8213/aaca97

Kitchatinov, L. L. (2022). Inferring quadrupolar dynamo mode from sunspot statistics. *Geomagnetism and Aeronomy*, *62*(7), 817–822. https://doi.org/10.1134/S0016793222070143

Korte, M., Donadini, F., & Constable, C. G. (2009). Geomagnetic field for 0–3 ka: 2. A new series of time-varying global models. *Geochemistry, Geophysics, Geosystems*, *10*(6), Q06008. https://doi.org/10.1029/2008GC002297

Krivova, N. A., & Solanki, S. K. (2002). The 1.3-year and 156-day periodicities in sunspot data: Wavelet analysis suggests a common origin. *Astronomy & Astrophysics*, *394*(2), 701–706. https://doi.org/10.1051/0004-6361:20021063

Lee, E. H., Ahn, Y. S., Yang, H. J., & Chen, K. Y. (2004). The sunspot and auroral activity cycle derived from Korean historical records of the 11th–18th century. *Solar Physics*, *224*(1–2), 373–386. https://doi.org/10.1007/s11207-005-5199-8

Lockwood, M., & Barnard, L. (2015). An arch in the UK. *Astronomy and Geophysics*, *56*(4), 4–25. https://doi.org/10.1093/astrogeo/atv132

Lockwood, M., Nevanlinna, H., Barnard, L., Owens, M. J., Harrison, R. G., Rouillard, A. P., & Scott, C. J. (2014). Reconstruction of geomagnetic activity and near-Earth interplanetary conditions over the past 167 yr–Part 4: Near-Earth solar wind speed, IMF, and open solar flux. In *Annales geophysicae* (Vol. 32, pp. 383–399). Copernicus Publications. https://doi.org/10.5194/angeo-32-383-2014

Lockwood, M., Owens, M. J., BarnardDavis, L. C. J., & Steinhilber, F. (2011). The persistence of solar activity indicators and the descent of the Sun into Maunder minimum conditions. *Geophysical Research Letters*, *38*(22), L22105. https://doi.org/10.1029/2011GL049811

Lomb, N. R. (1976). Least-squares frequency analysis of unequally spaced data. *Astrophysics and Space Science*, *39*(2), 447–462. https://doi.org/10.1007/BF00648343

Miyahara, H., Masuda, K., Muraki, Y., Furuzawa, H., Menjo, H., & Nakamura, T. (2004). Cyclicity of solar activity during the Maunder minimum deduced from radiocarbon content. *Solar Physics*, *224*(1–2), 317–322. https://doi.org/10.1007/s11207-005-6501-5

Nagovitsyn, Y. A. (2007). Solar cycles during the Maunder minimum. *Astronomy Letters*, *33*(5), 340–345. https://doi.org/10.1134/S1063773707050076

Nandy, D., Muñoz-Jaramillo, A., & Martens, P. C. (2011). The unusual minimum of sunspot cycle 23 caused by meridional plasma flow variations. *Nature*, *471*(7336), 80–82. https://doi.org/10.1038/nature09786

Ni, B., Thorne, R. M., Zhang, X., Bortnik, J., Pu, Z., Xie, L., et al. (2016). Origins of the Earth's diffuse auroral precipitation. *Space Science Reviews*, *200*(1–4), 205–259. https://doi.org/10.1007/s11214-016-0234-7

Owens, M. J., & Lockwood, M. (2012). Cyclic loss of open solar flux since 1868: The link to heliospheric current sheet tilt and implications for the Maunder minimum. *Journal of Geophysical Research*, *117*(A4), A04102. https://doi.org/10.1029/2011JA017193

Owens, M. J., Lockwood, M., & Riley, P. (2017). Global solar wind variations over the last four centuries. *Scientific Reports*, *7*(1), 41548. https://doi.org/10.1038/srep41548

Owens, M. J., Usoskin, I., & Lockwood, M. (2012). Heliospheric modulation of galactic cosmic rays during grand solar minima: Past and future variations. *Geophysical Research Letters*, *39*(19), L19102. https://doi.org/10.1029/2012GL053151

Passos, D., Nandy, D., Hazra, S., & Lopes, I. (2014). A solar dynamo model driven by mean-field alpha and Babcock-Leighton sources: Fluctuations, grand-minima-maxima, and hemispheric asymmetry in sunspot cycles. *Astronomy & Astrophysics*, *563*, A18. https://doi.org/10.1051/0004-6361/201322635

Poluianov, S. V., Usoskin, I. G., & Kovaltsov, G. A. (2014). Cosmogenic isotope variability during the Maunder Minimum: Normal 11-year cycles are expected. *Solar Physics*, *289*(12), 4701–4709. https://doi.org/10.1007/s11207-014-0587-6

Press, W. H., & Rybicki, G. B. (1989). Fast algorithm for spectral analysis of unevenly sampled data. *The Astrophysical Journal*, *338*, 277. https://doi.org/10.1086/167197

Ribes, J. C., & Nesme-Ribes, E. (1993). The solar sunspot cycle in the Maunder Minimum AD 1645 to AD 1715. *Astronomy and Astrophysics*, *276*, 549.

Riley, P., Lionello, R., Linker, J. A., Cliver, E., Balogh, A., Beer, J., et al. (2015). Inferring the structure of the solar corona and inner heliosphere during the Maunder Minimum using global thermodynamic magnetohydrodynamic simulations. *The Astrophysical Journal*, *802*(2), 105. https://doi.org/10.1088/0004-637X/802/2/105

Roy, S., Prasad, A., Panja, S. C., Ghosh, K., & Patra, S. N. (2019). A search 347 for periodicities in F10.7 solar radio flux data. *Solar System Research*, *53*(3), 224–232. https://doi.org/10.1134/S0038094619030031

Scargle, J. D. (1982). Studies in astronomical time series analysis. II. Statistical aspects of spectral analysis of unevenly spaced data. *The Astrophysical Journal*, *263*, 835–853. https://doi.org/10.1086/160554

Schlamminger, L. (1990). Aurora-borealis during the Maunder Minimum. *Monthly Notices of the Royal Astronomical Society*, *247*, 67.

Schröder, W. (1992). On the existence of the 11-year cycle in solar and auroral activity before and during the so-called Maunder Minimum. *Journal of Geomagnetism and Geoelectricity*, *44*(2), 119–128. https://doi.org/10.5636/jgg.44.119

Schüssler, M., & Cameron, R. H. (2018). Origin of the hemispheric asymmetry of solar activity. *Astronomy & Astrophysics*, *618*, A89. https://doi.org/10.1051/0004-6361/201833532

Shapiro, A. I., Schmutz, W., Rozanov, E., Schoell, M., Haberreiter, M., Shapiro, A. V., & Nyeki, S. (2011). A new approach to the long-term reconstruction of the solar irradiance leads to large historical solar forcing. *Astronomy & Astrophysics*, *529*, A67. https://doi.org/10.1051/0004-6361/201016173

Silverman, S. M. (1983). The visual aurora as a predictor of solar activity. *Journal of Geophysical Research*, *88*(A10), 8123–8128. https://doi.org/10.1029/JA088iA10p08123

Silverman, S. M. (1992). Secular variation of the aurora for the past 500 years. *Reviews of Geophysics*, *30*(4), 333–351. https://doi.org/10.1029/92RG01571

Sokoloff, D., & Nesme-Ribes, E. (1994). The Maunder Minimum: A mixed-parity dynamo mode? *Astronomy and Astrophysics*, *288*, 293–298.

Solanki, S. K., Krivova, N. A., Schüssler, M., & Fligge, M. (2002). Search for a relationship between solar cycle amplitude and length. *Astronomy & Astrophysics*, *396*(3), 1029–1035. https://doi.org/10.1051/0004-6361:20021436

Stephenson, F. R., & Willis, D. M. (2008). "Vapours like fire light" are Korean aurorae. *Astronomy and Geophysics*, *49*(3), 3–34. https://doi.org/10.1111/j.1468-4004.2008.49334.x

Temmer, M. (2021). Space weather: The solar perspective: An update to Schwenn (2006). *Living Reviews in Solar Physics*, *18*(1), 4. https://doi.org/10.1007/s41116-021-00030-3

Usoskin, I. G. (2017). A history of solar activity over millennia. *Living Reviews in Solar Physics*, *14*(1), 3. https://doi.org/10.1007/s41116-017-0006-9

Usoskin, I. G., Arlt, R., Asvestari, E., Hawkins, E., Käpylä, M., Kovaltsov, G. A., et al. (2015). The Maunder Minimum (1645–1715) was indeed a grand minimum: A reassessment of multiple datasets. *Astronomy & Astrophysics*, *581*, A95. https://doi.org/10.1051/00046361/201526652

Usoskin, I. G., Hulot, G., Gallet, Y., Roth, R., Licht, A., Joos, F., et al. (2014). Evidence for distinct modes of solar activity. *Astronomy & Astrophysics*, *562*, L10. https://doi.org/10.1051/0004-6361/201423391

Usoskin, I. G., Solanki, S. K., Krivova, N. A., Hofer, B., Kovaltsov, G. A., Wacker, L., et al. (2021). Solar cyclic activity over the last millennium reconstructed from annual 14C data. *Astronomy & Astrophysics*, *649*, A141. https://doi.org/10.1051/0004-6361/202140711

Vaquero, J. M., Kovaltsov, G. A., Usoskin, I. G., Carrasco, V. M. S., & Gallego, M. C. (2015). Level and length of cyclic solar activity during the Maunder minimum as deduced from the active-day statistics. *Astronomy & Astrophysics*, *577*, A71. The corresponding GSN deduced from the active-day statistics are publicly available at. https://doi.org/10.1051/0004-6361/201525962

Wang, Y., Chen, S., Xu, K., Yan, L., Yue, X., He, F., & Wei, Y. (2021). Ancient auroral records compiled from Korean historical books. *Journal of Geophysical Research: Space Physics*, *126*(1), e2020JA028763. https://doi.org/10.1029/2020JA028763

WDC-SILSO. (1620–1810). Group number series VERSION 1.0 [Dataset]. Royal Observatory of Belgium. https://www.sidc.be/SILSO/groupnumberv3

Willis, D. M., Stephenson, F. R., & Fang, H. (2007). Sporadic aurorae observed in East Asia. *Annales Geophysicae*, *25*(2), 417–436. https://doi.org/10.5194/angeo-25-417-2007

Willis, D. M., Stephenson, F. R., & Singh, J. R. (1996). Auroral observations on AD 1770 September 16: The earliest known conjugate sightings. *The Quarterly Journal of the Royal Astronomical Society*, *37*, 733.

Yau, K. K. C., Stephenson, F. R., & Willis, D. M. (1995). *A catalogue of auroral observations from China, Korea and Japan (193 BC-AD 1770)*. Rutherford Appleton Lab. ISSN 1358-6254 Retrieved from https://ui.adsabs.harvard.edu/abs/1995caof.book…Y

Yeates, A. R., Nandy, D., & Mackay, D. H. (2008). Exploring the physical basis of solar cycle predictions: Flux transport dynamics and persistence of memory in advection-versus diffusion-dominated solar convection zones. *The Astrophysical Journal*, *673*(1), 544–556. https://doi.org/10.1086/524352

Zhang, Z. W. (1985). Korean auroral records of the period AD 1507-1747 and the SAR arcs. *The Journal of the British Astronomical Association*, *95*, 205.

Zhu, F. R., & Jia, H. Y. (2018). Lomb–Scargle periodogram analysis of the periods around 5.5 year and 11 year in the international sunspot numbers. *Astrophysics and Space Science*, *363*(7), 1–4. https://doi.org/10.1007/s10509-018-3332-z